IET Nanobiotechnology

Research Article

Green synthesis of nanosilver-decorated graphene oxide sheets

ISSN 1751-8741
Received on 7th January 2015
Revised on 25th January 2016
Accepted on 18th February 2016
doi: 10.1049/iet-nbt.2015.0043
www.ietdl.org

Claramaría Rodríguez-González, Pamela Velázquez-Villalba, Pedro Salas, Víctor M. Castaño ✉

Centro de Física Aplicada y Tecnología Avanzada, Universidad Nacional Autónoma de México, Boulevard Juriquilla 3001, 76230 Juriquilla, Querétaro, México

✉ *E-mail: castano@fata.unam.mx*

Abstract: A green facile method has been successfully used for the synthesis of graphene oxide sheets decorated with silver nanoparticles (rGO/AgNPs), employing graphite oxide as a precursor of graphene oxide (GO), $AgNO_3$ as a precursor of Ag nanoparticles (AgNPs), and geranium (*Pelargonium graveolens*) extract as reducing agent. Synthesis was accomplished using the weight ratios 1:1 and 1:3 GO/Ag, respectively. The synthesised nanocomposites were characterised by scanning electron microscopy, transmission electron microscopy, atomic force microscopy, X-ray diffraction, UV-visible spectroscopy, Raman spectroscopy, energy dispersive X-ray spectroscopy and thermogravimetric analysis. The results show a more uniform and homogeneous distribution of AgNPs on the surface of the GO sheets with the weight ratio 1:1 in comparison with the ratio 1:3. This eco-friendly method provides a rGO/AgNPs nanocomposite with promising applications, such as surface enhanced Raman scattering, catalysis, biomedical material and antibacterial agent.

1 Introduction

Graphene, a new form of carbon consisting of a 2D single layer of carbon atoms bonded in a hexagonal structure, has attracted important attention due to their distinguished thermal, chemical, mechanical and electrical properties [1]. The planar structure of graphene creates a unique arrangement of extended sheet with both sides accessible, providing a remarkably high surface area [2, 3]. Graphene oxide (GO) is an oxygen-rich graphene sheet that possesses important mechanical properties, antibacterial activity and biocompatibility, depending on its concentration, surface functionalisation and other factors [4–6]. The abundance of functionalities such as epoxide, carboxylic, carbonyl and hydroxyl groups on the surface of GO facilitates its dispersibility. Likewise, such functional groups act as nucleation sites for the growth of diverse nanostructures [7, 8]. These unique properties make GO an ideal matrix to supporting and dispersing metal nanoparticles, obtaining new hybrid materials with enhanced properties as a result of a cooperative interaction [5, 9, 10].

Silver nanoparticles (AgNPs) have chemical stability and distinctive optical, electrical and catalytic properties. From a biological perspective, the surface/volume ratio facilitates the interaction with microorganisms, making them an effective antibacterial, antiviral, and fungicidal agent [11, 12]. Recent evidence suggested that AgNPs possess anti-inflammatory and antitumor effect, attracting a wide range of application [13, 14]. GO sheets decorated with AgNPs exhibit enhanced electrical, thermal and antibacterial properties, which leads to interesting applications, such as surface enhanced Raman spectroscopy, catalytic activity, biomedical material and antibacterial agent [15, 16].

Several physical and chemical methods have been reported for the synthesis of rGO/AgNPs nanocomposites, among them the chemical-reduction route. However, these procedures usually involve the use of hazardous stabilisers, solvents or reducing agents, such as hydrazine, sodium borohydride and formaldehyde, which pollute the environment or hamper their further biomedical applications [15, 17–19]. Green synthesis is an alternative to avoid these inconveniences, which comprise the use of eco-friendly solvents, non-toxic chemical or environment safe reducing agents. The cost-effective, environment-friendly and simplicity are some advantages for green synthesis, although has drawbacks, including the problems to control the morphology and distribution of the nanoparticles [20–22]. Moreover, plant extracts are an alternative to be used both as reducing and stabilising agents in the synthesis of nanoparticles [22]. Thus far, green synthesis of graphene/AgNPs nanohybrids have been extensively investigated. However, to the best of our knowledge, few studies have reported green synthesis of rGO/AgNPs nanocomposite by using plant extracts [20–26].

Geranium (*Pelargonium graveolens*), an aromatic plant widely cultivated, presents anticancer, anti-inflammatory and wound healing properties [27]. In addition, the geranium leaf extract exhibits reducing properties, which has been already investigated for the green synthesis of AgNPs [28, 29]. In this context, we would like to contribute with a rGO/AgNPs nanocomposite synthesised by a green approach without the use of toxic chemicals, and thus increase its possible biotechnological applications. Taking advantage of non-toxicity, availability, cost-effective and biocompatibility, we explore the use of the geranium leaf extract as a green reducing agent for the synthesis of rGO/AgNPs nanocomposite, studying the effect of two weight ratios of GO/Ag. This approach allows the reduction of graphene oxide and silver salts simultaneously and provides a homogeneous distribution of AgNPs on GO sheet using the weight ratio 1:1.

2 Experimental

2.1 Materials

Graphite flakes (12'' × 0.120'') were purchased from Electron Microscopy Science. Silver nitrate ($AgNO_3$, 99.9999%), ethanol (EtOH), sulphuric acid (H_2SO_4, 98%), potassium permanganate ($KMnO_4$, 99%), hydrogen peroxide (H_2O_2, 35%) and hydrochloric acid (HCl, 37%) were supplied by Sigma Aldrich. Geranium extract was obtained in the laboratory from fresh leaves of *P. graveolens*.

2.2 Synthesis of graphite oxide

Graphite oxide was prepared from the flake graphite according to the modified Hummers method [30]. Briefly, 6 g of graphite powder was

added to 135 ml H_2SO_4 in an ice bath. Then $KMnO_4$ was gradually added with stirring, maintaining the temperature below 20°C for some minutes and at 35°C for 2 h. The mixture was diluted with 98 ml of deionised water, and the reaction was increased to 98°C. A H_2O_2 solution was added to remove permanganate excess. The solid product was centrifuged and washed repeatedly with 5% HCl solution. At last, the suspension was dried in a vacuum oven at 60°C for 24 h to obtain graphite oxide.

2.3 Preparation of the geranium extract

The fresh green leaves of the geranium (*P. graveolens*) were washed several times with deionised water to remove unwanted dust particles. Then 12.15 g of washed leaves with 100 ml of deionised water were boiled in a three-neck flask for 15 min. The leaf aqueous extract was filtered and stored for its further use.

2.4 Synthesis of graphene oxide sheets decorated by AgNPs

The rGO/AgNPs were synthesised using the weight ratios 1:1 and 1:3 GO/Ag, respectively. Graphite oxide powder was dispersed in 15 ml of deionised water by ultrasonication for 2 h, forming stable GO suspension. After GO with 40 ml of EtOH were added in a three-neck flask with stirring at 60°C. The geranium extract was added slowly to the mixture with magnetic stirring for 5 min. Subsequently, a 27 mm $AgNO_3$ solution was added by slow drip, maintaining stirring for 45 min. Finally, the products were washed with deionised water by centrifugation (12,000 rpm for 15 min), and the resulting rGO/AgNPs were dried in vacuum oven at 60°C for 24 h. The samples were labelled as rGO/AgNPs 1:1 and rGO/AgNPs 1:3, respectively. For a weight ratio of 1:1 were used 30 mg of GO, 30 mg of Ag and 20 ml of geranium extract, and for the ratio 1:3 were added 15 mg of GO, 45 mg of Ag and 30 ml of geranium extract.

2.5 Characterisation

UV-visible (UV-vis) spectra were recorder in a range between 200–800 nm using a DR 5000 Uv-Vis Spectrophotometer (Hach, Canada). Local chemical analysis from GO and AgNPs in the nanocomposites was performed with energy dispersive X-ray spectroscopy (EDS) with an Oxodor Inca X-Sight attached to a scanning electron microscopy (SEM, JEOL, JSM-6060 LV), where the morphology was studied too. For transmission electron microscopy (TEM), a JEOL JEM-1010 was operated at an accelerating voltage of 60–80 kV. Information about topography of GO and nanocomposites was analysed by atomic force microscopy (AFM), realised in AFM, 5000-Angstrom Advanced. Raman spectra were recorded in a Dilor, Labram II spectrometer with a 488 nm Argon laser excitation and an integration time of 5 and 60 s using 30 mW. Raman spectra were recorder in a range between 500 and 2500 cm^{-1}. X-ray diffraction (XRD) patterns were recorded by a Rigaku, Miniflex+ powder diffractometer with Cu kα radiation (λ = 0.154 Å). The recorded XDR patterns were obtained from 5° to 80° (2θ). Thermal stability of the nanocomposites was studied by a thermogravimetric analyser (TGA, SDT Q600, DSC-TGA Standard) with a heating rate of 10°C/min under a nitrogen atmosphere.

3 Results and discussion

3.1 Uv-vis spectra analysis

Uv-vis spectra was employed to monitor the formation of GO and rGO/AgNPs nanocomposites as shown in Fig. 1. The GO dispersion spectrum exhibits a maximum at 230 nm, which correspond to the electronic π–π* transitions of C–C aromatic bonds, and a shoulder at 305 nm assigned to the *n*–π* transitions of C=O bonds [16, 31, 32]. In the rGO/AgNPs 1:1 nanocomposite, the absorption peak of GO dispersion at 230 nm gradually red-shifted to 254 nm and the absorption peak at 300 nm disappeared, indicating a possible restoration of the electronic conjugation sp^2 within GO network [16, 33, 34].

The formation of AgNPs is confirmed by the presence of absorption peak at ~447 nm, which is characteristic of the surface plasmon resonance of AgNPs [15, 35, 36]. Furthermore, in the case of rGO/AgNPs 1:3 nanocomposite the characteristic absorption peak of the AgNPs is located at ~406 nm. The shift toward a shorter wavelength suggests the presence of small metallic nanoparticles. However, GO sheets are decorated with large clusters of AgNPs as can be seen in TEM analysis section as detailed below. This AgNPs clusters could be associated with a high concentration of Ag precursor, which promotes the formation of cores and small nanoparticles. Its subsequent growth tend to form nanoparticles clusters or agglomerates. Moreover, a decrease in the concentration of GO regarding to Ag, facilitates AgNPs agglomeration according to previous reports. In addition the peak associated with aromatic C–C bonds was only slightly shifted,

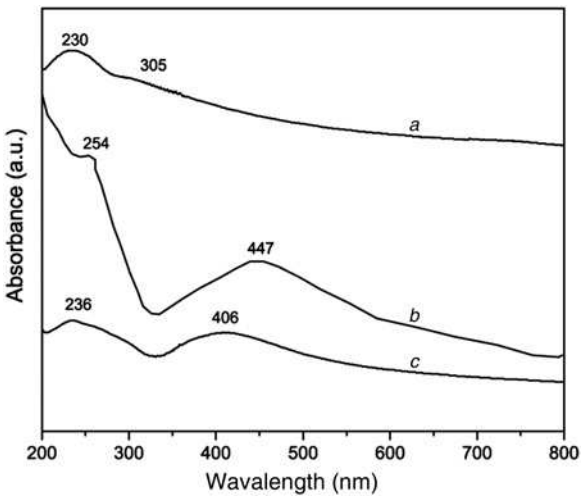

Fig. 1 *Uv-vis absorption spectra of*
a GO and rGO/AgNPs with the weight ratio
b 1:1
c 1:3

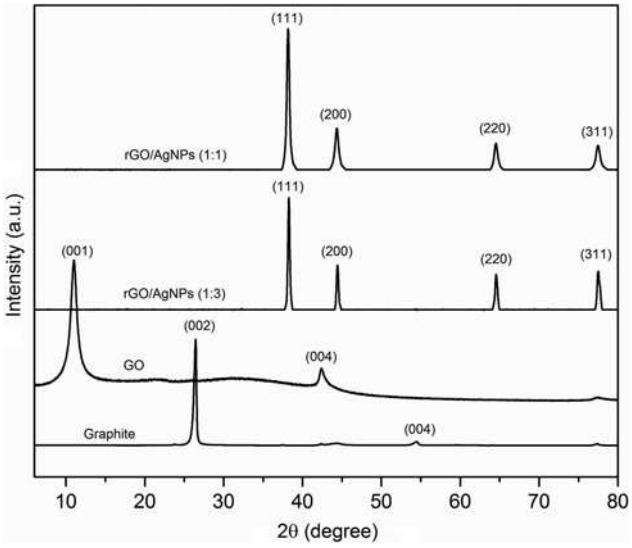

Fig. 2 *XRD pattern of graphite, GO, rGO/AgNPs 1:1 and rGO/AgNPs 1:3*

which could be related to a minor restoration of the graphitic network [37, 38].

3.2 X-ray diffraction

XRD patterns of graphite, GO and hybrid materials are shown in Fig. 2. Graphite has a sharp and intense diffraction peak at $2\theta = 26.6°$ corresponding to (002) plane, which is characteristic of the high crystallinity of the material. The XRD of GO exhibits a peak at $2\theta = 10.7°$ corresponding to (001) plane associated with an interlayer spacing of 8.3 Å. The GO has a larger interlayer spacing than graphite plane (3.4 Å) due to the oxygen functional groups containing on GO sheet [33].

For the rGO/AgNPs 1:1 and 1:3 nanocomposite, the peaks at 38.1°, 44.3°, 64.5° and 77.5° are assigned to the (111), (200), (220) and (311) planes of the AgNPs face centred cubic (FCC) crystal structure, confirming its presence. The peaks of the planes are consistent with the standard card (JCPDS No. 87–0597) and indicate that the nanoparticles are composed of pure Ag crystal without the presence of another phase. The average crystallite sizes were obtained by using Scherrer's formula

$$D = \frac{(0.9)\lambda}{\beta \cos(\theta)} \quad (1)$$

Here, λ is the X-ray wavelength, β is the corrected half-width of the strongest diffraction peak, and θ is the diffraction angle. The crystallite size for rGO/AgNPs 1:1 sample is 3.66 nm and for rGO/AgNPs 1:3 sample is 5.32 nm. These results are consistent with TEM observations. Moreover, in the diffraction pattern of the nanocomposites, the absence of a peak in GO indicates that the assembly of AgNPs can prevent the restacking of graphene sheets. These changes suggest the reduction and functionalisation with AgNPs of the GO [39–41].

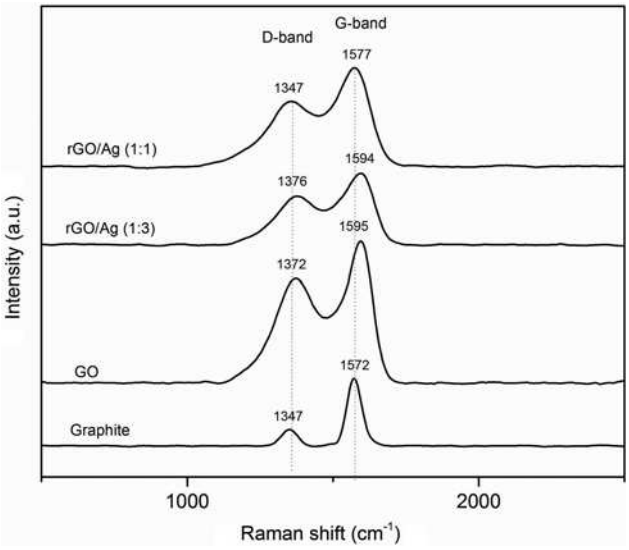

Fig. 3 *RAMAN spectra of graphite, GO, rGO/AgNPs 1:1 and rGO/AgNPs 1:3*

Table 1 Position of *D* and *G* bands and I_D/I_G values of graphite, graphene oxide, and the nanocomposites rGO/AgNPs 1:1 and 1:3 obtained by Raman spectroscopy

Sample	*D* band position, cm^{-1}	*G* band position, cm^{-1}	I_D/I_G
Graphite	1347	1572	0.26
graphene oxide	1372	1595	1.03
rGO/AgNPs (1:1)	1347	1577	0.83
rGO/AgNPs (1:3)	1376	1594	0.84

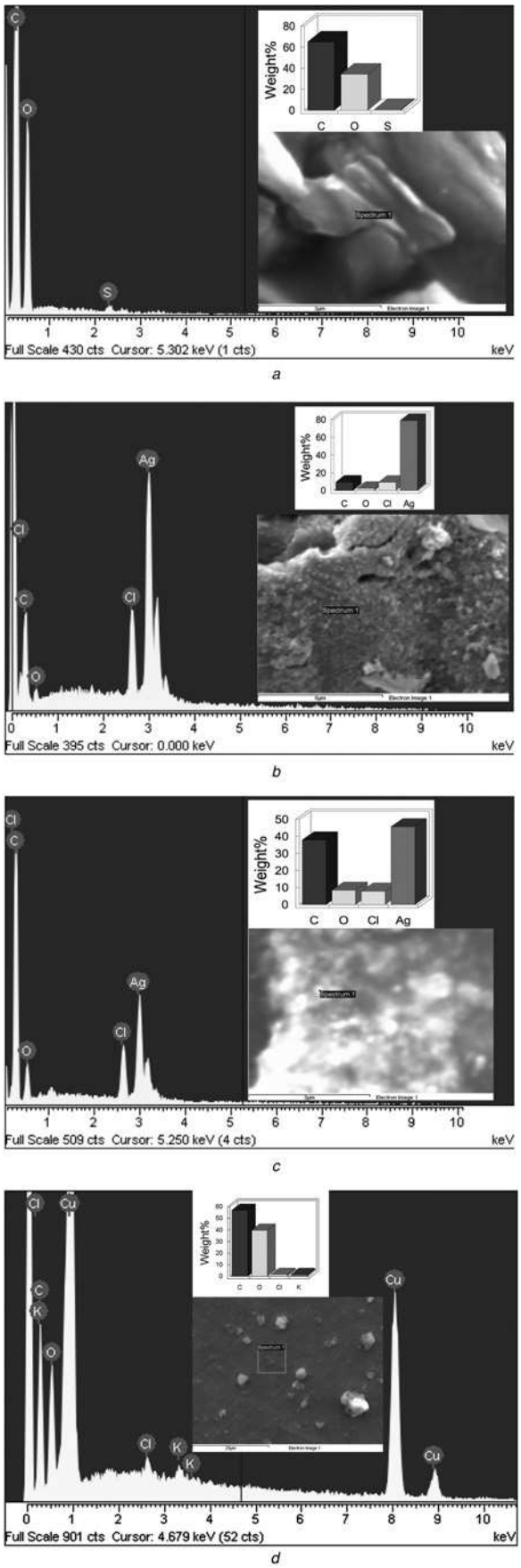

Fig. 4 *EDS spectrum of*

a GO
b rGO/AgNPs 1:1
c rGO/AgNPs 1:3 and geranium extract
d Geranium extract

3.3 Raman spectra analysis

Fig. 3 shows the Raman spectra of graphite, GO and rGO/AgNPs nanocomposites. Graphite exhibits a weak peak located at approximately 1347 cm^{-1} called *D*-band, and a sharp and well-defined peak at 1572 cm^{-1} called the *G*-band. The *D*-band is attributed to the defects and disorder of carbon atoms, whereas the *G*-band is associated with the vibration in the plane of sp^2-hybridisation of carbon atoms [42, 43]. After oxidation, the *D*-band intensity increases significantly and is shifted to a higher wave number (1372 cm^{-1}), and the *G*-band is broadened and shifted to ~1595 cm^{-1}. The increased intensity of the *D*-band could be due to the significant size reduction of the sp^2 domains, and the presence of defects associated with the functional groups attachment on carbon sheets [44].

When the graphene sheets are decorated with silver nanoparticles, specifically in the rGO/AgNPs 1:1 hybrid material, the *D* and *G* bands undergo a shift towards fewer wave numbers compared with those observed in the GO localised to 1347 and 1577 cm^{-1}, respectively (Table 1). This behaviour can be associated to the strong interaction of the AgNPs with GO sheets [40]. In the case of the rGO/AgNPs 1:3 hybrid material, *D* and *G* bands have a slightly displaced indicating an ineffective functionalisation.

The intensity ratio of *D* and *G* bands is used to determine the degree of graphitic disorder. Thus, GO exhibits a ratio I_D/I_G of 1.03, whereas for rGO/AgNPs 1:1 and 1:3 is 0.83 and 0.84, respectively. The decrease in the intensities ratio *D*/*G* suggesting the partial restoration of the graphitic network in the GO attributed probably to the reduction process made through the decoration with AgNPs. Similar results have been reported for various metal nanoparticles and metal oxides [15, 45–47].

3.4 Energy dispersive X-ray spectroscopy

EDS was used to determine the elements quantity in rGO and rGO/AgNPs nanocomposites. EDS of GO sheets is shown in Fig. 4*a*, the resulting chemical composition exhibits the presence of the *C* (65.04 wt%) and *O* (34.29 wt%) elements. The sulphur element appears as a waste product from the concentrated H_2SO_4 used in the oxidation reaction. The EDS spectrum of rGO/AgNPs 1:1 and 1:3 nanocomposites indicates the presence of *C*, *O*, *C*l and Ag elements. The percentage of Ag in the nanocomposites was 78.93 wt% for rGO/AgNPs 1:1 (Fig. 4*b*) and 45.78 wt% for rGO/AgNPs 1:3 (Fig. 4*c*). The additional chlorine is associated to the chemical composition of the plant extract. Fig. 4*d* presents the EDS spectrum of the geranium extract, revealing the presence of *C*, *O*, *C*l and *K*.

The strong signal energy peaks for Ag atoms in 3 keV confirms the AgNPs formation on the surface of the GO sheets [48].

3.5 TEM analysis

The morphology and size distribution of the GO and nanocomposites were examined by TEM, as shown in Fig. 5. The GO sheets (Fig. 5*a*) exhibit large lateral dimensions and a translucent, wavy and wrinkled appearance. The TEM micrograph of rGO/AgNPs 1:1 nanocomposite (Fig. 5*b*) shows a uniform distribution of AgNPs on the surface of the GO sheets. The size of the nanoparticles, however, shows a relatively broad distribution, indicating that the reduction is affected by the interaction with the GO sheets. The AgNPs have a predominantly spherical shape. The absence of nanoparticles outside the GO surface indicates a good interaction with the support [49]. In contrast, in the rGO/AgNPs 1:3 nanocomposite (Fig. 5*c*) the AgNPs

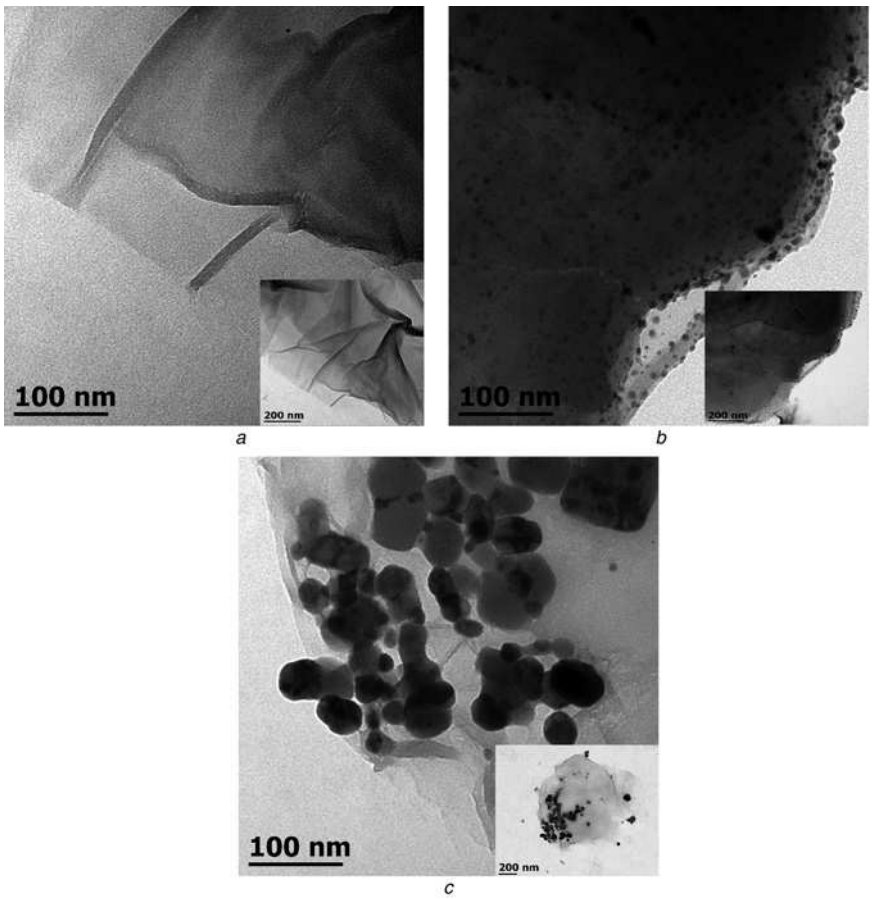

Fig. 5 *TEM images of*

a GO
b rGO/AgNPs 1:1
c rGO/AgNPs 1:3

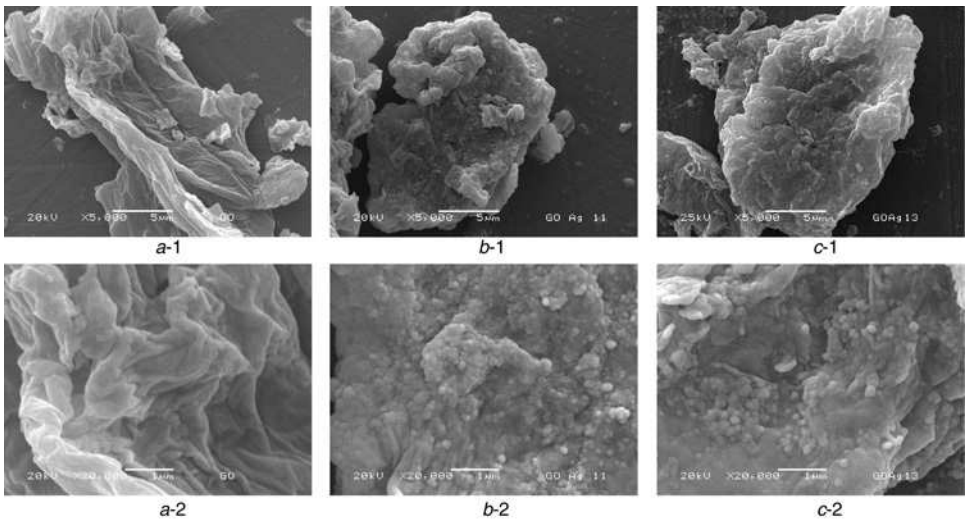

Fig. 6 *SEM images of*

a-1 GO

b-1 rGO/AgNPs 1:1

c-1 rGO/AgNPs 1:3 at 5000×, and (*a*-2), (*b*-2) and (*c*-2) are their respectively zooms at 20000×

form large agglomerates, which are composed of small nanoparticles. This could be due to higher silver content in this sample, favouring its accumulation [50]. A more detailed microscopy analysis, including high resolution TEM and AFM imaging, will be reported separately.

3.6 SEM analysis

In Fig. 6 SEM micrographs showed clustering of soft and clean GO sheets which characteristic waves and wrinkles. The morphology is different for GO/AgNPs 1:1 and 1:3 nanocomposites (Figs. 6*b* and *c*) where SEM images illustrate the presence of a large amount of nanoparticles deposited on the GO causing its rough appearance and demonstrating its successful surface modification [50]. The effect to use two different weight ratios is mostly observed in the distribution and size of AgNPs. In rGO/AgNPs 1:1 (Figs. 6*b*-1, *b*-2), AgNPs are well distributed on the rGO sheets with approximately the same size. Moreover, in rGO/AgNPs 1:3 nanocomposite (Figs. 6*c*-1, *c*-2), AgNPs tend to agglomerate, which is consistent with TEM observations [6].

3.7 AFM analysis

AFM in non-contact mode was used to evaluate the thickness and surface roughness in GO and rGO/AgNPs 1:1. The AFM images of GO (Fig. 7*a*) revealed the presence of flakes with an average height of 1.31 nm and the lateral dimensions in the range of several nanometres to micrometres. The thickness in the range of 1–2 nm is associated with the complete exfoliation of the sheets

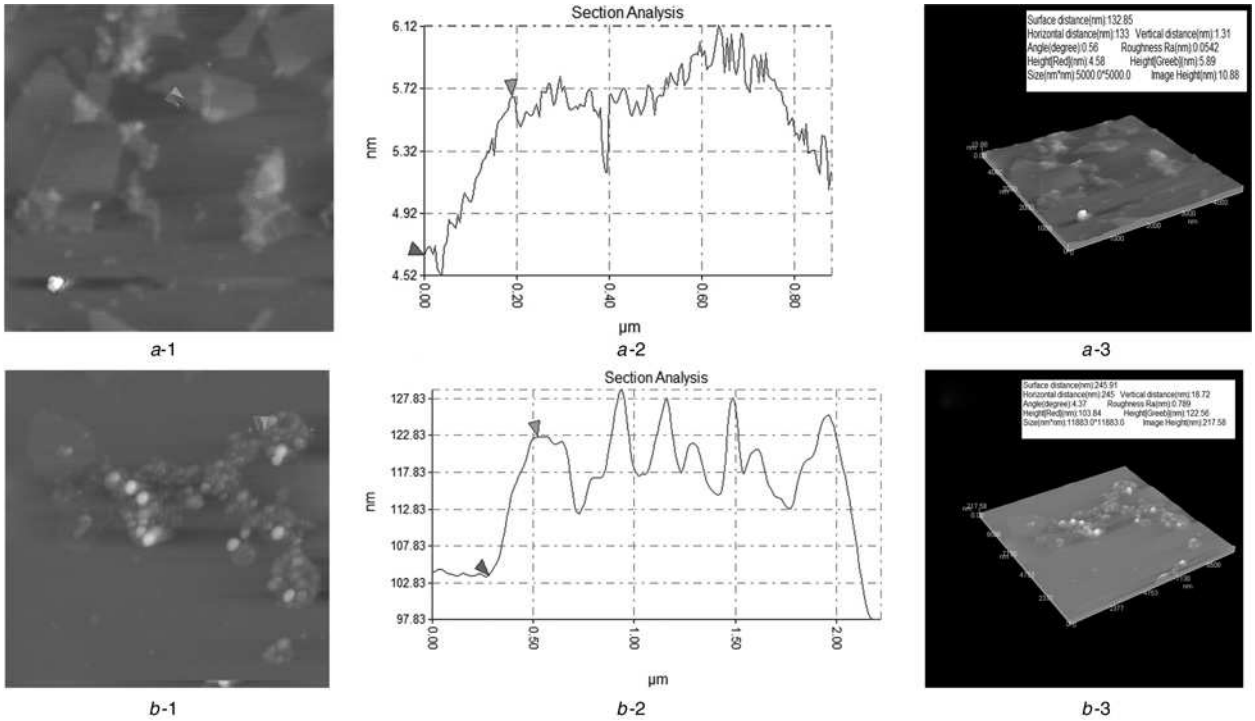

Fig. 7 *AFM images of*

a-1 GO

b-1 rGO/AgNPs 1:1, its corresponding graphics (*a*-2) and (*b*-2), and its AFM 3D images (*a*-3) and (*b*-3)

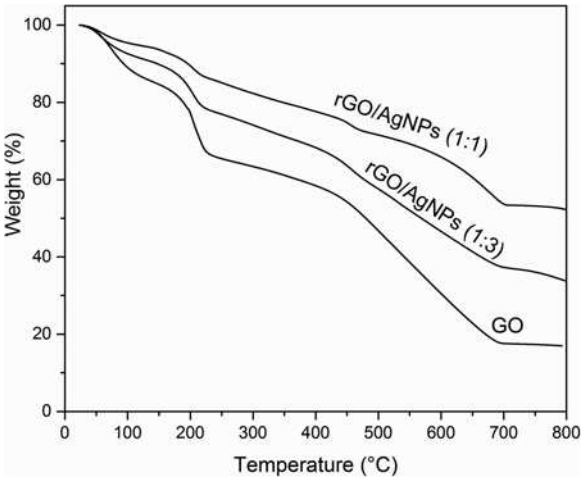

Fig. 8 *TGA curves of GO, rGO/AgNPs 1:1 and rGO/AgNPs 1:3*

[51, 52]. Fig. 7*b* clearly illustrates the wide presence of AgNPs as bright spots on the GO sheets, which is consistent with TEM and SEM analysis for the same nanocomposite. In addition, the thickness of the sheet increases to 18.72 nm (Fig. 7*b*-2) confirming the anchorage of metal nanoparticles on graphene flakes.

3.8 TGA analysis

TGA curves of GO and hybrid material were shown in Fig. 8. The first degradation step of GO occurred around 160°C and 240°C with a 15% of weight loss, corresponding to the loss of polar groups on the GO sheets, whereas in the nanocomposites occurred at around 190°C. The weight loss of 37% between 440°C and 690°C, is resulted from pyrolysis of the carbon skeleton. Accordingly, the total weight loss in GO is around 66% (between 150°C and 690°C).

The rGO/AgNPs nanocomposite has an obvious weight loss of 4% (rGO/AgNPs 1:1) and 6% (rGO/AgNPs 1:3) between 190°C and 240°C due to pyrolysis of the labile oxygen-containing functional groups [53]. Furthermore, the weight loss between 440°C and 690°C has an important decrease in the rGO/AgNPs 1:1 and 1:3 nanocomposites of 20 and 25%, respectively. In rGO/AgNPs 1:1 the total weight loss was 37% between 190°C and 690°C, whereas in rGO/AgNPs 1:3 was 46%. The different values in the total weight loss could be due to a better distribution of the AgNPs on the GO sheets. The decrease in the total weight loss in the nanocomposite in comparison with GO confirms the successful synthesis of rGO/AgNPs nanocomposite [54].

4 Conclusions

GO sheets decorated with AgNPs were synthesised by a simple, sustainable and environmental friendly method using geranium (*P. graveolens*) extract as eco-friendly reducing agent with medium reaction conditions, generating AgNPs with single crystalline phase. The oxygen-rich functional groups allowed the chemical anchoring of the nanoparticles and its conducive distribution on the GO sheets. The results indicated that the optimal conditions for the synthesis of rGO/AgNPs were achieved with a weight ratio of 1:1 of GO/Ag, in which the GO sheets show a homogeneous distribution of AgNPs. This environmentally friendly method avoids the use of any additional chemical. Hence, considering the aforementioned properties of Ag and GO, the rGO/AgNPs nanocomposite has important potential to be exploited in biomedical applications.

5 Acknowledgments

The authors wish to thank for technical support: Ma. Lourdes Palma Tirado (TEM), Francisco Rodríguez Melgarejo (RAMAN), Beatriz Milán Malo (XDR), Karen Yael Castrejon (TGA), Alicia del Real López and C. Peza-Ledesma (SEM, EDS). Claramaría Rodríguez-González is recipient of a postdoctoral fellowship from DGAPA/UNAM. This article is dedicated to the memory of Mr. Juan Carlos Velázquez Ramírez.

6 References

1 Goenka, S., Sant, V., Sant, S.: 'Graphene-based nanomaterials for drug delivery and tissue engineering', *J. Control. Release*, 2014, **173**, pp. 75–88
2 Zhang, L., Zhang, F., Yang, X., *et al.*: 'Porous 3D graphene-based bulk materials with exceptional high surface area and excellent conductivity for supercapacitors', *Sci. Rep.*, 2013, **3**, p. 108
3 He, G., Wu, H., Ma' K., *et al.*: 'Photosynthesis of multiple valence silver nanoparticles on reduced graphene oxide sheets with enhanced antibacterial activity', *Synth. React. Inorg. Metal-Org. Nano-Metal Chem.*, 2013, **43**, (4), pp. 440–445
4 Chook, S., Chia, C., Zakaria, S., *et al.*: 'Antibacterial performance of Ag nanoparticles and AgGO nanocomposites prepared via rapid microwave-assisted synthesis method', *Nanoscale Res. Lett.*, 2012, **7**, (1), pp. 541–547
5 Pinto, A., Gonçalves, I., Magalhães, F.: 'Graphene-based materials biocompatibility: a review', *Colloids Surf. B, Biointerfaces*, 2013, **111**, pp. 188–202
6 Nguyen, V., Kim, B., Jo, Y., *et al.*: 'Preparation and antibacterial activity of silver nanoparticles-decorated graphene composites', *J. Supercritical Fluids*, 2012, **72**, pp. 28–35
7 Stankovich, S., Piner, R., Nguyen, S., *et al.*: 'Synthesis and exfoliation of isocyanate-treated graphene oxide nanoplatelets', *Carbon*, 2006, **44**, (15), pp. 3342–3347
8 Ji, Z., Shen, X., Xu, Y., *et al.*: 'Anchoring noble metal nanoparticles on CeO2 modified reduced graphene oxide nanosheets and their enhanced catalytic properties', *J. Colloid Interface Sci.*, 2014, **432**, pp. 57–64
9 Goncalves, G., Marques, P., Granadeiro, C., *et al.*: 'Surface modification of graphene nanosheets with gold nanoparticles: the role of oxygen moieties at graphene surface on gold nucleation and growth', *Chem. Mater.*, 2009, **21**, (20), pp. 4796–4802
10 Guo, S., Dong, S.: 'Graphene nanosheet: synthesis, molecular engineering, thin film, hybrids, and energy and analytical applications', *Chem. Soc. Rev.*, 2011, **40**, (5), pp. 2644–2672
11 Lara, H., Ayala-Nuñez, N., Ixtepan-Turrent, L., *et al.*: 'Mode of antiviral action of silver nanoparticles against HIV-1', *J. Nanobiotechnology*, 2012, **8**, (1), pp. 1–10
12 Rai, M.K., Deshmukh, S.D., Ingle, A.P., *et al.*: 'Silver nanoparticles: the powerful nanoweapon against multidrug-resistant bacteria', *J. Appl. Microbiol.*, 2012, **112**, (5), pp. 841–852
13 Wong, K., Liu, X.: 'Silver nanoparticles—the real ''silver bullet'' in clinical medicine?', *Med. Chem. Commun.*, 2010, **1**, (2), pp. 125–131
14 Gurunathan, S., Han, J.W., Park, J.H., *et al.*: 'Reduced graphene oxide-silver nanoparticle nanocomposite: a potential anticancer nanotherapy', *Int. J. Nanomed.*, 2015, **10**, pp. 6257–6276
15 Zainy, M., Huang, N.M., Kumar, S.V., *et al.*: 'Simple and scalable preparation of reduced graphene oxide-silver nanocomposites via rapid thermal treatment', *Mater. Lett.*, 2012, **89**, pp. 180–183
16 Hsu, K.-C., Chen, D.-H.: 'Green synthesis and synergistic catalytic effect ofAg/reduced graphene oxide nanocomposite', *Nanoscale Res. Lett.*, 2014, **9**, (1), p. 484
17 Lightcap, I.V., Kosel, T.H., Kamat, P.V.: 'Anchoring semiconductor and metal nanoparticles on a two-dimensional catalyst mat. storing and shuttling electrons with reduced graphene oxide', *Nano Lett.*, 2010, **10**, (2), pp. 577–583
18 Li, C., Wang, X., Chen, F., *et al.*: 'The antifungal activity of graphene oxide-silver nanocomposites', *Biomaterials*, 2013, **34**, (15), pp. 3882–3890
19 Joshi, C.A., Markad, B.G., Haram, K.S.: 'Rudimentary simple method for the decoration of graphene oxide with silver nanoparticles: their application for the amperometric detection of glucose in the human blood samples', *Electrochim. Acta*, 2015, **161**, pp. 108–114
20 Iravani, S.: 'Green synthesis of metal nanoparticles using plants', *Green Chem.*, 2011, **13**, pp. 2638–2650
21 Zhang, D., Liu, X., Wang, X.: 'Green synthesis of graphene oxide sheets decorated by silver nanoprisms and their anti-bacterial properties', *J. Inorg. Biochem.*, 2011, **105**, (9), pp. 1181–1186
22 Mittal, A., Chisti, Y., Banerjee, U.: 'Synthesis of metallic nanoparticles using plant extracts', *Biotechnol. Adv.*, 2010, **31**, (2), pp. 346–356
23 Wang, Z., Xu, C., Li, X., *et al.*: 'In situ green synthesis of Ag nanoparticles on tea polyphenols-modified graphene and their catalytic reduction activity of 4-nitrophenol', *Colloids Surf. A, Physicochem. Eng. Aspects*, 2015, **485**, pp. 102–110
24 Gurunathan, S., Han, J.W., Park, J.H., *et al.*: 'Reduced graphene oxide-silver nanoparticl nanocomposite: a potential anticancer nanotherapy', *Int. J. Nanomed.*, 2015, **10**, pp. 6257–6276
25 Barua, S., Thakur, S., Aidew, L., *et al.*: 'One step preparation of a biocompatible antimicrobial reduced graphene oxide-silver nanohybrid as a tropical antimicrobial agent', *RSC Adv.*, 2014, **4**, (19), pp. 9777–9783
26 Al-Marri, H.A., Khan, M., Khan, M.: 'Pulicaria glutinosa extract: a toolbox to synthesize highly reduced graphene oxide-silver nanocomposites', *Int. J. Mol. Sci.*, 2015, **16**, (1), pp. 1131–1142
27 Charles, D.J.: 'Geranium' 'Antioxidant properties of spices, herbs and other sources' (Springer, 2013, 1st edn.), pp. 329–334
28 Pandian, M., Marimuthu, R., Natesan, G., *et al.*: 'Development of biogenic silver nanoparticle from *Pelargonium graveolens* leaf extract and their antibacterial activity', *Am. J. Nanosci. Nanotechnol.*, 2013, **1**, (2), pp. 57–64

29 Shankar, S., Ahmad, A., Sastry, M.: 'Geranium leaf assisted Biosynthesis of silver nanoparticles', *Biotechnol. Prog.*, 2003, **19**, pp. 1627–1631
30 Hummers, W.S., Offman, R.E.: 'Preparation of graphitic oxide', *J. Am. Chem. Soc.*, 1958, **80**, (6), pp. 1339–1339
31 Zhu, C., Guo, S., Fang, Y., *et al.*: 'Reducing sugar: new functional molecules for the green synthesis of graphene nanosheets', *ACS Nano*, 2010, **4**, (4), pp. 2429–2437
32 Baby, T.T., Ramaprabhu, S.: 'Synthesis and nanofluid application of silver nanoparticles decorated graphene', *J. Mater. Chem.*, 2011, **21**, pp. 9702–9709
33 Yuan, W., Gu, Y., Li, L.: 'Green synthesis of graphene/Ag nanocomposites', *Appl. Surf. Sci.*, 2012, **261**, pp. 753–758
34 Das, M., Sarma, R., Saikia, R., *et al.*: 'Synthesis of silver nanoparticles in an aqueous suspension of graphene oxide sheets and its antimicrobial activity', *Colloids Surf. B, Biointerfaces*, 2011, **83**, pp. 16–22
35 Bhui, D., Bar, H., Sarkar, P., *et al.*: 'Synthesis and UV-vis spectroscopic study of silver nanoparticles in aqueous SDS solution', *J. Mol. Liq.*, 2009, **145**, pp. 33–37
36 Xu, Z., Gao, H., Gouxin, H.: 'Solution-based synthesis and characterization of silver nanoparticle-graphene hybrid film', *Carbon*, 2011, **49**, pp. 4731–4738
37 Singh, M., Titus, E., Krishna, R., *et al.*: 'Direct nucleation of silver nanoparticles on raphene sheet', *J. Nanosci. Nanotechnol.*, 2012, **12**, pp. 1–6
38 Muszynski, R., Seger, B., Kamat, P.: 'Decorating graphene sheets with gold nanoparticles', *J. Phys. Chem. C.*, 2008, **112**, (4), pp. 5263–5266
39 Li, Y., Cao, Y., Xie, J., *et al.*: 'Facile solid-state synthesis of Ag/graphene oxide nanocomposites as highly active and stable catalyst for the reduction of 4-nitrophenol', *Catal. Commun.*, 2014, **58**, pp. 21–25
40 Tian, Y., Wang, F., Liu, Y., *et al.*: 'Green synthesis of silver nanoparticles on nitrogen-doped graphene for hydrogen peroxide detection', *Electrochim. Acta*, 2014, **146**, pp. 646–653
41 Kima, K.-S., Kimb, I.-J., Parka, S.-J.: 'Influence of Ag doped graphene on electrochemical behaviors and specific capacitance of polypyrrole-based nanocomposites', *Synth. Met.*, 2010, **160**, pp. 2355–2360
42 Shen, J., Yan, B., Ma, H., *et al.*: 'One step hydrothermal synthesis of TiO_2-reduced graphene oxide sheets', *J. Mater. Chem.*, 2011, **21**, pp. 3415–3421
43 Wojtoniszak, M., Chen, X., Kalenczuk, R.J., *et al.*: 'Synthesis, dispersion, and cytocompatibility of graphene oxide and reduced graphene oxide', *Colloids Surf. B, Biointerfaces*, 2012, **89**, pp. 79–85
44 Wang, X., Dou, W.: 'Preparation of graphite oxide (GO) and the thermal stability of silicone rubber/GO nanocomposites', *Thermochimica Acta*, 2012, **529**, pp. 25–28
45 Wang, H., Tian, H., Wang, S., *et al.*: 'Simple and eco-friendly solvothermal synthesis of luminescent reduced graphene oxide small sheets', *Mater. Lett.*, 2012, **78**, pp. 170–173
46 Luo, Z., Yuwen, L., Han, Y., *et al.*: 'Reduced graphene oxide/PAMAM-silver nanoparticles nanocomposite modified electrode for direct electro chemistry of glucose oxidase and glucose sensing', *Biosensors and Bioelectronics*, 2012, **36**, pp. 179–185
47 Tabrizi, M.A., Varkani, J.N.: 'Green synthesis of reduced graphene oxide decorated with gold nanoparticles and its glucose sensing application', *Sensors and Actuators B*, 2014, **202**, pp. 475–482
48 Nisha, S.N., Aysha, O.S., Rahaman, S.N., *et al.*: 'Lemon peels mediated synthesis of silver nanoparticles and its antidermatophytic activity', *Spectrochimica Acta A Mol. Biomol. Spectrosc.*, 2014, **124**, pp. 194–198
49 Phama, T., Choib, B., Lima, K., *et al.*: 'A simple approach for immobilization of gold nanoparticles on graphene oxide sheets by covalent bonding', *Applied Surface Science*, 2011, **257**, pp. 3350–3357
50 Li, J., Kuang, D., Feng, Y., *et al.*: 'Green synthesis of silver nanoparticles-graphene oxide nanocomposite and its application in electrochemical sensing of tryptophan', *Biosens. Bioelectron.*, 2013, **42**, pp. 198–206
51 Shen, J., Shi, M., Yan, B., *et al.*: 'One-pot hydrothermal synthesis of Ag-reduced graphene oxide composite with ionic liquid', *J. Mater. Chem.*, 2011, **21**, pp. 7795–7801
52 Zhou, L., Gu, H., Wang, C., *et al.*: 'Study on the synthesis and surface enhanced Raman spectroscopy of graphene-based nanocomposites decorated with noble metal nanoparticles', *Colloids Surf. A, Physicochem. Eng. Aspects*, 2013, **430**, pp. 103–109
53 Yang, Y., Liu, T.: 'Fabrication and chatacterization of graphene oxide/zinc oxide nanorods hybrid', *Appl. Surf. Sci.*, 2011, **257**, pp. 8950–8954
54 Han, Y., Luo, Z., Yuwen, L., *et al.*: 'Synthesis of silver nanoparticles on reduced graphene oxide under microwave irradiation with starch as an ideal reductant and stabilizer', *Appl. Surf. Sci.*, 2013, **226**, pp. 188–193